A Non-premixed Hydrogen Combustion Process Using a Spark-Ignited Hydrogen Jet

Anne Beyer[1], Hans-Jürgen Berner[2], André Casal Kulzer[1,2]

[1]IFS Institute of Automotive Engineering Stuttgart
Automotive Powertrain Systems
University of Stuttgart
Pfaffenwaldring 12
70569 Stuttgart
anne.beyer@ifs.uni-stuttgart.de

[2]FKFS
Research Institute for Automotive Engineering and Powertrain Systems Stuttgart
Pfaffenwaldring 12
70569 Stuttgart

Abstract: The general prognosis expects a significant impact of hydrogen on the energy and transport sector in the upcoming years. Due to a century of experience in combustion engine development, the transition to hydrogen fuel serves as a promising contribution to the defossilisation of the transport sector. Several ongoing research projects focus on homogeneous lean engine operation to suppress NO_X emissions. Among the challenges of this concept is the high boost pressure demand to produce a significant power output. In contrast, this paper addresses the potential of a stoichiometric combustion process. A single-cylinder research engine on a hydrogen test bench forms the basis for the stationary experimental investigations. The hydrogen direct injection starts just before the firing top dead center to prevent premixing and, thereby, related pre-reactions or knocking. The jet gets ignited by a conventional spark plug before the end of injection. The injection duration and the maximum injector mass flow strongly influence the combustion duration. The experiments also show an effect of the ignition timing on the heat release rate and the pressure rise in the combustion chamber. For stoichiometric engine operation, the non-premixed combustion is beneficial in terms of engine-out NO_X emissions compared to the homogeneous mode. Nevertheless, both strategies lead to higher NO_X emissions than the lean operation. Still, the authors see potential in the presented operation mode when coupled with catalytic conversion using hydrogen as a reducing agent.

1 Introduction

Recently presented engine concepts and demonstrator vehicles generally focus on the lean combustion of gaseous hydrogen with a significant advantage in NO_X engine-out emissions [1, 2]. Nevertheless, stoichiometric operation facilitates reaching high engine loads with a reduced boost pressure level. Among the challenges of stoichiometric hydrogen combustion are the fast laminar burning velocities of hydrogen in air and the low minimum ignition energy compared to gasoline, favoring abnormal combustion like pre-ignition or knocking [3]. A possible mitigation strategy is the application of a combustion moderator, e.g., EGR or water injection, discussed in [4].

The approach of this study strives for a reduced risk of abnormal combustion by avoiding the premixing of hydrogen and air in the combustion chamber. Injection of the hydrogen and ignition by the spark plug start shortly before TDCF to force a highly stratified combustion. The subsequently introduced fuel jet converts in mixing controlled mode until the end of injection. [5] investigated an SOI variation with the ignition timing fixed at TDCF in an optical test engine. The authors discovered significant differences in flame propagation and HRR for igniting either shortly after SOI, in the center of the injection, at the end or shortly afterwards. Especially for lean combustion, the so-called tail ignition at the end of injection was beneficial for the combustion stability. In contrast to this approach, the present study looks into a constant SOI with an ignition timing during the early injection to focus on minimum time for premixing. The rail pressure is a relevant parameter for the intended combustion strategy, in which injection continues during combustion. The fact that the rail pressure, or more precisely the pressure at the injector nozzle, should at least be higher than the maximum pressure in the combustion chamber determines the hydrogen pressure demand for the described combustion process.

2 Methodology

A hydrogen engine test bench operated under stationary conditions delivers data for this study to gain knowledge about the fundamental correlations of the described combustion process.

2.1 Experimental Setup

The single-cylinder research engine, derived from a Mercedes-Benz M 254 passenger car engine, uses a spray-guided gasoline combustion process. The outward-opening Bosch HDEV4 piezo-controlled gasoline injector sits vertically, close to the center of the combustion chamber roof, and the spark plug is positioned between the intake and exhaust valves [6]. Recently, several research projects used this gasoline injector as an interim solution for H_2 DI with intake or compression stroke injection, compensating for the low hydrogen injector mass flow with a longer injection duration [7]. For non-premixed combustion, this limits the achievable maximum engine load concerning a reasonable combustion duration. Aside from that, the engine operates on a conventional gasoline single-spark ignition system with an iridium spark plug.

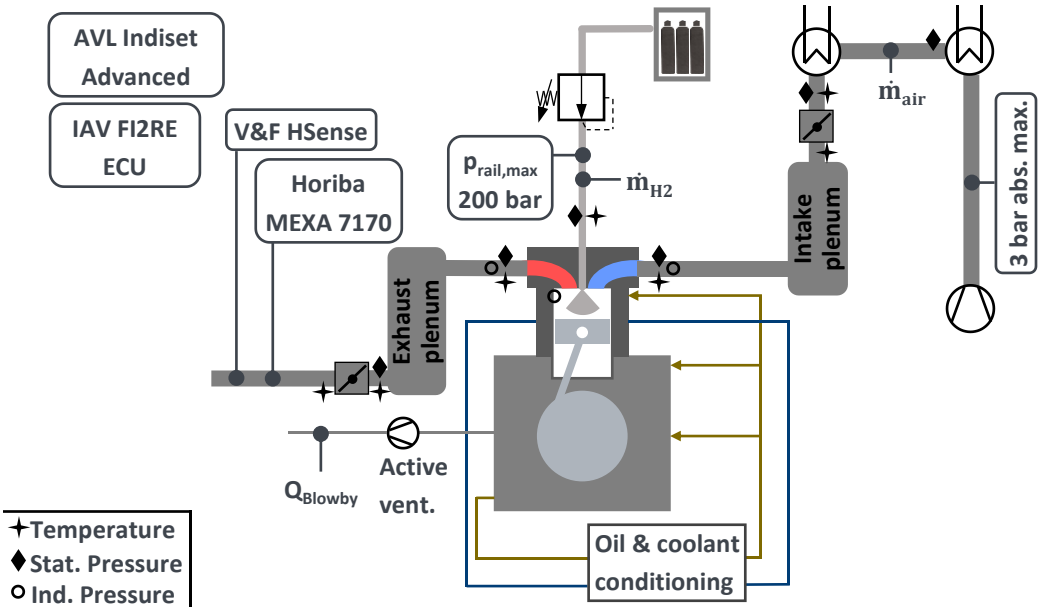

Figure 1: Schematic test bench setup

Figure 1 illustrates the test and measurement equipment of the experimental setup. Hydrogen comes from 300 bar bottle bundles, and the adjustable pressure regulator enables a maximum rail pressure of 200 bar. A Coriolis mass flow meter measures the stationary hydrogen mass flow to the engine. As a precaution, an active ventilation system provided by Hengst reduces the hydrogen concentration in the crankcase whenever hydrogen blow-by occurs. Kistler pressure sensors in the intake manifold, combustion chamber and exhaust manifold, combined with an AVL Indicom system, serve for the combustion analysis. An external charging unit and a conditioning system control the boundary conditions of the intake air. A throttle flap reduces pulsations in the intake air path and enables throttled operating points at low engine load. An exhaust flap offers the possibility to adjust the resulting exhaust back pressure. The Horiba MEXA system measures the concentration of the conventional exhaust gas components, and the V&F HSense detects the H_2 concentration as a product of incomplete combustion in the exhaust system. The following equations, Eq. 2-1 and Eq. 2-2, published in [1], deliver the calculated air-to-fuel equivalency ratio considering the exhaust gas composition. The products of incomplete combustion influence the corrected oxygen content in the exhaust gas.

$$\lambda = \frac{[O_{2,\mathrm{corr}}] - 1}{4.7733 \cdot [O_{2,\mathrm{corr}}] - 1} \qquad \text{Eq. 2-1}$$

$$[O_{2,\mathrm{corr}}] = \frac{[O_{2,\mathrm{incom}}] + \frac{1}{2}[CO_{\mathrm{incom}}] - \frac{1}{2}[H_{2,\mathrm{incom}}] + \frac{21}{200}[NO_{X,\mathrm{incom}}] + [CO_{2,\mathrm{incom}}] - 410 \cdot 10^{-6}}{1 + \frac{1}{40}[NO_{X,\mathrm{incom}}] - \frac{1}{2}[CO_{\mathrm{incom}}] - \frac{3}{2}[H_{2,\mathrm{incom}}]}$$

Eq. 2-2

2.2 Experimental Conditions

The maximum hydrogen mass flow through the injector is a limiting factor for this test setup. Hence, an operation point with a low load of around 5 bar IMEP and a low engine speed of 1500 min^{-1} enables short injection durations considering the low nozzle cross-section. Additionally, the resulting low maximum cylinder pressures ease operating close to the limit of the maximum cylinder pressure gradient. The investigated parameters of the stoichiometric non-premixed combustion are injection and ignition timing, rail pressure and injector needle lift. The intake pressure and temperature are kept constant at 595 mbar and 40 °C, and the exhaust flap stays open.

As discussed in section 1, the hydrogen rail pressure is an important variable influencing the injection duration and the combustion quality in jet-guided mode. Both investigated pressure levels, 80 bar and 190 bar, still enable supercritical conditions for a near 5 bar IMEP operating point with maximum cylinder pressures of about 35 bar. Two different injector needle lifts for each rail pressure level additionally influence the injection duration. Particular interest lies in comparing a high rail pressure with a low needle lift and a low rail pressure with a high needle lift because they lead to an identical injection duration. For the variation of SOI for each case, the ignition angle matches the SOI angle. In a subsequent test, the SOI is kept constant for all cases, and an incrementally increased delay between injection and ignition illustrates the effects of premixing and local mixture conditions at the spark plug. The investigated cases are listed below with their abbreviated designations:

- **LP LL:** Low rail pressure (80 bar) and low injector needle lift
- **LP HL:** Low rail pressure (80 bar) and high injector needle lift
- **HP LL:** High rail pressure (190 bar) and low injector needle lift
- **HP HL:** High rail pressure (190 bar) and high injector needle lift.

3 Results and Discussion

Figure 2 shows the cylinder pressure, heat release rate, and integrated heat release for rail pressures of 80 bar and 190 bar with a low and high injector needle lift for 200 averaged cycles each. The colored bars represent the injection duration, and the arrows mark the ignition timing.

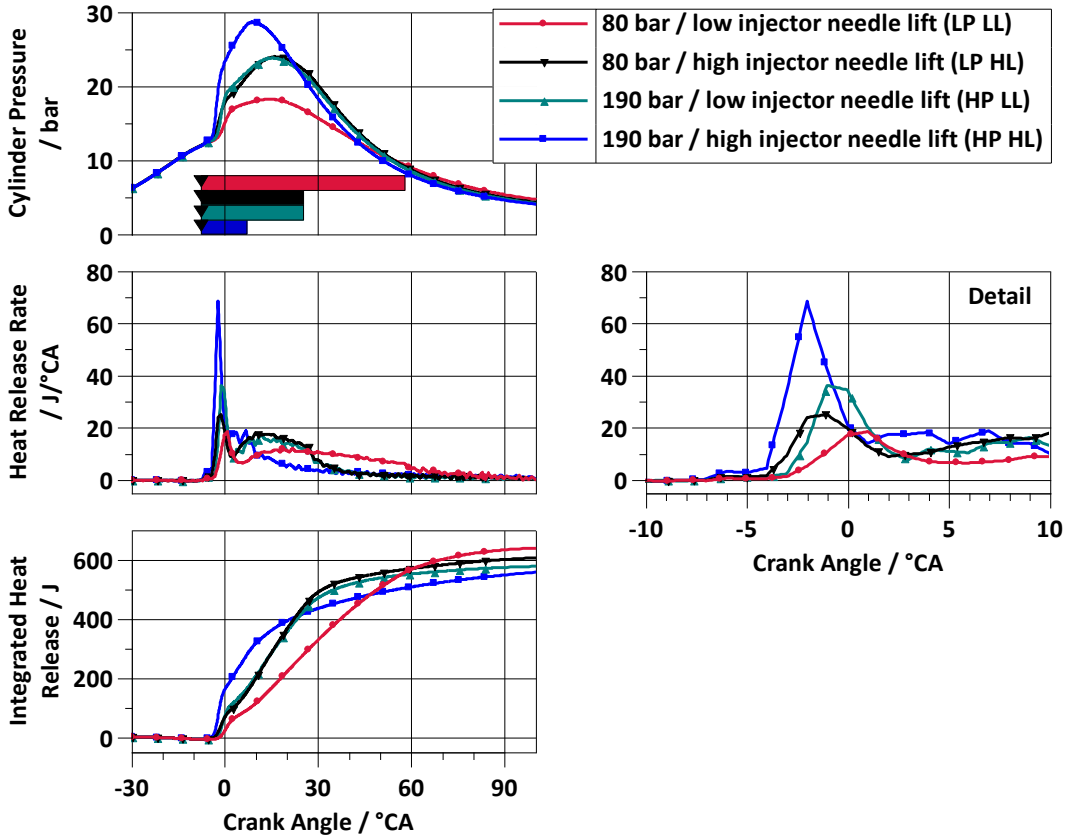

Figure 2: Cylinder pressure, heat release rate and integrated heat release for a variation of rail pressure and injector needle lift

The SOI and ignition timing are kept constant at 8 °CA bTDCF for all options. Fast fuel conversion occurs for the high rail pressure and needle lift because of the lowest initial air-to-fuel equivalency ratio at the spark plug position. The detailed view of the heat release rate on the right side of Figure 2 clarifies the distinctive premixed share and the early start of combustion, especially for this high mass flow configuration. The corresponding steep increase in integrated heat release around TDCF, in combination with high flame speed and small quenching distance, indicates a high potential for wall heat losses.

Either the combination of high rail pressure and low needle lift or low rail pressure and high needle lift results in the same injection duration. That leads to similar behavior in the heat release for both options. The detailed view on the right shows a higher initial heat release rate for the higher rail pressure. A reason for this might be the higher turbulence of the jet generated through higher pressure at the injector nozzle. The experiment with the low rail pressure and low needle lift shows a slow initial reaction but reaches the maximum integrated heat release through the long combustion duration.

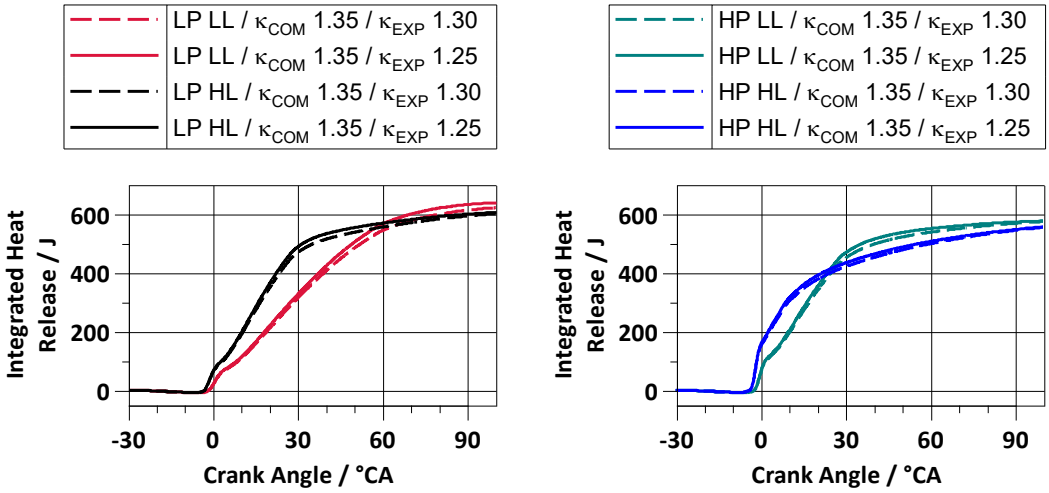

Figure 3: Influence of the polytropic index on integrated heat release

The investigated cases pose a challenge for calculating the mass fraction burned out of the integrated heat release. For this study, the Hohenberg equation (Eq. 3-1) delivers the heat release rate using a linear interpolated polytropic index from the compression value to the expansion value.

$$\Delta Q_{1-2} = \frac{1}{\kappa - 1} \cdot V_2 \cdot \left[p_2 - p_1 \cdot \left(\frac{V_1}{V_2} \right)^{\kappa} \right] \qquad \text{Eq. 3-1}$$

The interpolation occurs within the preset crank angle window for the heat release calculation. Therefore, a variation of the calculation window influences the polytropic index for a specific crank angle. The presented comparison of rail pressure and injector needle lift requires a wide calculation window to illustrate the slow combustion of the LP LL option. The chosen calculation window starts at 30 °CA bTDCF and ends at 100 °CA aTDCF.

The recommended values for a gasoline DI engine of 1.35 for compression and 1.30 for expansion lead to a slow increase towards the maximum of the integrated heat release for all four cases, especially for the HP HL experiment. In the first place, the polytropic index of the expansion is lowered to 1.25 to possibly inhibit an implausible further increase in the integrated heat release after the end of combustion. Figure 3 compares the integrated heat release calculated using the default or adjusted values. The adjusted polytropic index leads to a higher gradient of the linear part of the curves.

To quantify the differences, Table 1 lists the different crank angle positions in °CA aTDCF for 50 % mass fraction burned and the durations in °CA to release 10 to 90, 10 to 50, or 50 to 90 % of the maximum energy. The values of MFB50 and MFB50-10 are similar for the different polytropic indices of all cases. Deviations from the MFB90 of 3 to 5 °CA arise for the LP HL, HP LL, and HP HL cases. Still, the long combustion duration of the HP HL case seems implausible considering the belonging early end of injection. A further possibility could be to consider the temperature dependency of the polytropic index by calculating a varying value for each crank angle of the working cycle. Because of the deviant local air-to-fuel equivalency ratios at the spark plug, this could have a strong influence on the calculated burn duration of the investigated cases. Furthermore, the cylinder pressure oscillations resulting from igniting the jet in the investigated setup are worth mentioning because they affect the calculation of the HRR. Therefore, considering the filtering or smoothing of the cylinder pressure signal is reasonable. The shown results are calculated without filtering or smoothing but with a sampling frequency of 1 °CA and subsequent averaging of the 200 working cycles. A comparison of the different methods is subject to further analysis.

Table 1: Comparison mass fraction burned for investigated cases and polytropic indices

	LP LL	LP HL	HP LL	HP HL	κ_{COM} / κ_{EXP}
MFB50 /	29	16	16	7	1.35 / 1.30
°CA aTDCF	29	16	16	7	1.35 / 1.25
MFB90-10	60	52	47	62	1.35 / 1.30
/ °CA	59	46	42	59	1.35 / 1.25
MFB50-10	26	17	16	10	1.35 / 1.30
/ °CA	26	16	16	10	1.35 / 1.25
MFB90-50	34	35	31	52	1.35 / 1.30
/ °CA	33	29	26	49	1.35 / 1.25

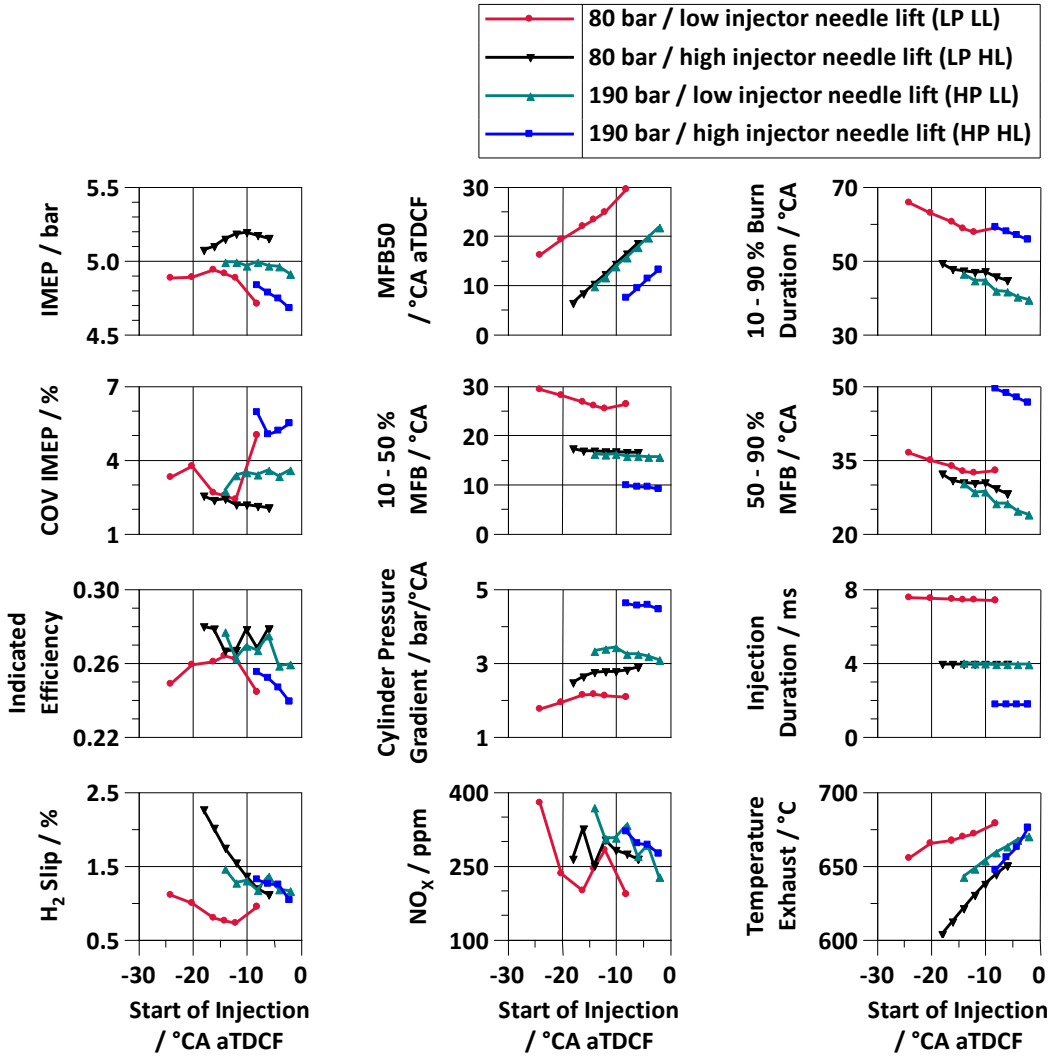

Figure 4: Variation of the start of injection for two different rail pressures and injector needle lifts

Figure 4 shows graphs for relevant time-averaged measurements plotted over SOI. A high cylinder pressure gradient and an unstable, inefficient combustion are associated with high rail pressure and needle lift operation. In contrast, the low rail pressure and needle lift produce the lowest cylinder pressure gradient and H_2 slip. The beneficial hydrogen conversion during the long combustion duration results in high exhaust gas temperature but doesn't bring an efficiency advantage. High and low injector mass flows show a difference between the most efficient points of MFB50. The high mass flow experiment with a fast initial fuel conversion favors early positions of MFB50 around 4 °CA aTDCF, while the low mass flow leads to later optimum points of MFB50 around 15 °CA aTDCF.

The most promising option for this operation point is 80 bar rail pressure with a high injector needle lift because it delivers maximum efficiency and the most stable combustion with the lowest coefficients of variance. This study doesn't reveal distinct differences in the engine-out NO_X emissions of the investigated cases. Worth mentioning is that all options produce an approximately five times lower concentration than the homogeneous stoichiometric operation. One of the reasons for that might be the locally rich conditions around the spark plug for non-premixed jet-guided operation. On the other hand, the homogeneous lean operation above $\lambda = 2.4$ delivers single-digit NO_X ppm values for a comparable operating point.

Figure 5 shows the subsequent variation of ignition timing for all investigated cases with a constant SOI of 8 °CA bTDCF. The effect of the higher premixed share through later ignition timing appears in every graph. The later start of combustion, in combination with similar late burning phases, shortens the combustion duration. In particular, the HRR approximates the trend of homogeneous operation for the HP HL case with the latest ignition timing. Still, the curve reveals a slow late combustion phase like the other two ignition timing options. For all cases, the later ignition timings induce higher indicated efficiency and higher cylinder pressure gradients.

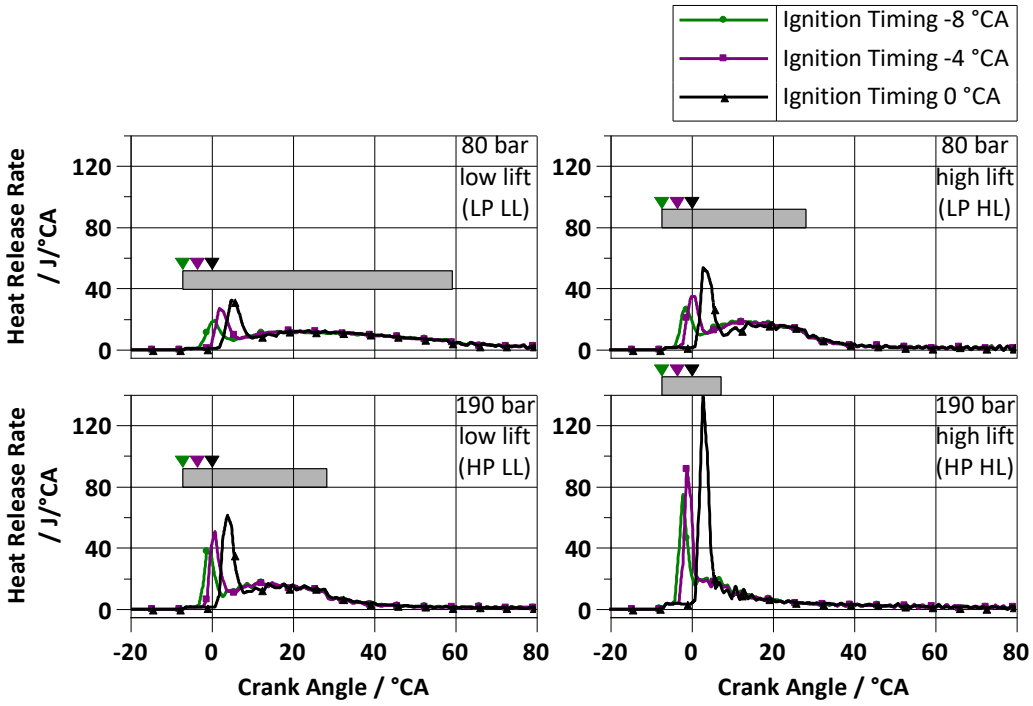

Figure 5: Heat release rate for a variation of ignition timing and two different rail pressures and injector needle lifts

Especially for the HP HL option, the cylinder pressure rise approximates the maximum value of around 8 bar/ °CA, considering combustion noise mitigation. In this regard, the low pressure or low lift options allow for later ignition timings that involve shorter combustion durations. An interesting subsequent experiment could be to compare the given options with an ignition timing after the injection of a similar fuel mass. For an equitable comparison, the SOI should be shifted for the different cases to ensure efficiency-optimized MFB50 positions.

4 Summary and Conclusion

This study illustrates the influence of the injector mass flow and the ignition timing for a hydrogen DI combustion process with a spark-ignited jet. The outward-opening gasoline injector suits fundamental investigations of jet-guided combustion at low engine speeds and loads. The findings can be summarized as follows:

- A variation of rail pressure and injector needle lift, and thereby a variation of the injector mass flow, influences the fraction of premixed combustion through deviating local air-to-fuel equivalency ratios at the spark plug at spark timing.
- The end of injection marks the point of the transition from mixing-controlled combustion to the late burning phase. The choice of the polytropic index impacts the calculated HRR for the late combustion phase and, thereby, both the calculated MFB90 and the calculated burn duration.
- An increase in the delay between the start of injection and ignition affects the premixed share of the combustion and, thereby, the cylinder pressure rise and the combustion duration.

For the presented test setup, the LP HL option shows the most promising results for this low load and engine speed operation point. The combustion process provides an advantage in engine-out NO_X emissions compared to the homogeneous stoichiometric operation but implicates significant energy loss through H_2 slip into the exhaust system. These losses are acceptable only if the H_2 slip helps reduce NO_X tailpipe emissions, e.g., by applying the selective catalytic conversion with H_2 suggested in [8]. Alternatively, [4] proposes the combination of a three-way catalyst with H_2 as a reduction agent and a downstream passive SCR system to convert the residual NO_X and NH_3.

This study illustrates the feasibility of a non-premixed stoichiometric strategy igniting the early hydrogen jet for the investigated operating point. An extension towards more points of the engine map and exhaust gas aftertreatment considerations are the subject of further experiments and analysis.

Reference List

[1] D. Lejsek et al., "Mixture Formation and Combustion in a Passenger Car Engine with Low Pressure H2 Direct Injection," in *19th Symposium „Sustainable Mobility, Transport and Power Generation"*, Graz, 2023.

[2] J. N. Geiler et al., "H2 Engine Hybrid Powertrain for Future Light Commercial Vehicles," in *10. International Engine Congress*, Baden-Baden, 2023.

[3] H.L. Yip et al., "A Review of Hydrogen Direct Injection for Internal Combustion Engines: Towards Carbon-Free Combustion," *Applied Sciences,* vol. 9, no. 22, p. 4842, 2019, doi: 10.3390/app9224842..

[4] P. Kapus et al., "Hydrogen for Internal Combustion Engines – a Viable Alternative for Passenger Car Propulsion," in *19th Symposium „Sustainable Mobility, Transport and Power Generation"*, Graz, 2023.

[5] M. K. Roy et al., "High-Pressure Hydrogen Jet and Combustion Characteristics in a Direct-Injection Hydrogen Engine," *SAE Int. J. Fuels Lubr.,* vol. 5, no. 3, pp. 1414-1425, 2012.

[6] O. Vollrath et al., "The New Mercedes-Benz In-line Six-cylinder Gasoline Engine with 48-V Electrification," *MTZ Worldwide,* no. 79, pp. 54-61, 2018, doi: 10.1007/s38313-018-0015-7.

[7] D. Lejsek et al., "Thermodynamic analysis of hydrogen engines with port fuel- and direct injection," in *18th Symposium „Sustainable Mobility, Transport and Power Generation"*, Graz, 2021.

[8] M. Borchers et al., "Selective Catalytic Reduction with Hydrogen for Exhaust gas after-treatment of Hydrogen Combustion Engines," *Topics in Catalysis,* no. 66, pp. 973-984, 2023, doi: 10.1007/s11244-022-01723-1.

Acknowledgements

The presented single-cylinder hydrogen engine study forms part of an international research project (FVV project no. 1446) performed by the Institute of Automotive Engineering (IFS) at University of Stuttgart under the direction of Prof. André Casal Kulzer and by the Automotive Powertrain Technologies Group of Dr. Patrik Soltic at Swiss Federal Laboratories for Materials Science and Technology (Empa). Based on a decision taken by the German Bundestag, it was supported by the Federal Ministry for Economic Affairs and Climate Action (BMWK) and the AIF (German Federation of Industrial Research Associations e.V.) within the framework of the collective research networking (CORNET) program (IGF/CORNET-No. 307 EN). Furthermore, it was financially supported by Swiss Federal Office of Energy (SI/502205-01) and FVV e.V. (funding no. 6014462). The project was conducted by a working group led by Dr. Stephan Liebsch (IAV GmbH). The authors gratefully acknowledge the support received from the funding organizations, from the FVV e.V. and from all those involved in the project.

Abbreviations

bTDCF/ aTDCF – Before/ After top dead center firing

°CA – Degree crank angle

DI – Direct injection

EGR – Exhaust gas recirculation

HP HL/ LL – High rail pressure and high/ low injector needle lift

HRR – Heat release rate

IMEP – Indicated mean effective pressure

LP HL/ LL – Low rail pressure and high/ low injector needle lift

MFBxx – xx % mass fraction burned

ppm – Parts per million

SOI - Start of injection